

# Design of new giant magnetostrictive structures for double-nut ball screw pre-tightening

Qingdong Wang<sup>1,2</sup> · Mingxing Lin<sup>1,2</sup>

Received: 5 July 2016 / Accepted: 17 March 2017 / Published online: 28 March 2017  
© The Brazilian Society of Mechanical Sciences and Engineering 2017

**Abstract** As a high-precision drive mechanism, double-nut ball screw is widely used in machining and manufacturing field. A pre-tightening structure added to the double-nut ball screw may reduce the axial clearance between nuts and screw, thus to increase transmission accuracy. The present commonly used pre-tightening structure cannot realize automatic regulation of pre-tightening force, so three new structures are designed in this article to achieve timely adjustment of pre-tightening force, namely the pre-tightening structure composed of hollow cylindrical GMM (Giant Magnetostrictive Material: Terfenol-D), the pre-tightening structure composed of three discrete Terfenol-D rods and the giant magnetostrictive pre-tightening structure with hinge-levers. After analyzing their structure characteristics and electromagnetic coupling relations, it is found that the giant magnetostrictive pre-tightening structure with hinge-levers is superior to the other two in performance. Electromagnetic coupling experiment result of this structure shows that it meets the pre-tightening requirements of double-nut ball screw, and can adjust the pre-tightening force by adjusting the electric current.

**Keywords** Double-nut ball screw · Pre-tightening · Giant magnetostrictive structure

Technical Editor: Aline Souza de Paula.

✉ Mingxing Lin  
mxlin@sdu.edu.cn

<sup>1</sup> School of Mechanical Engineering, Shandong University, Jinan 250061, China

<sup>2</sup> Key Laboratory of High Efficiency and Clean Mechanical Manufacture of Ministry of Education, Shandong University, Jinan 250061, China

## 1 Introduction

Ball screw is widely used in machining center, and its performance directly affects the numerical control machine's working accuracy and machining quality [1].

The ball screw axial clearance refers to the original clearance between nuts and the nut displacement. Usually a pre-tightening structure is added to ball screw to control the elastic deformation within the minimum limit, which can decrease the axial clearance and improve the ball screw's axial rigidity [2, 3].

The ball screw pre-tightening force is a key parameter affecting friction torque [4, 5]. Timely adjustment of pre-tightening force makes the ball screw rapidly adapt to high-acceleration start–stop, external load changes, temperature changes, etc.

## 2 Design of giant magnetostrictive structure for double-nut ball screw pre-tightening

### 2.1 Present double-nut ball screw pre-tightening structure

Currently, there are two kinds of ball screw pre-tightening methods: single nut and double nut. The double-nut method, which can repeatedly adjust and maintain the pre-tightening force, is used in precision transmission where the return clearance is not allowed to exist.

Double-nut pre-tightening methods include the gasket method, the thread method, the tooth difference method, the spring method and the piezoelectric ceramics method.

In the gasket method, the two nuts are separated by a gasket and contact with the screw in opposite direction.

A representative gasket pre-tightening method is mentioned in China patent document CN203656087U, which is shown in Fig. 1, where 1. screw, 2. assistant nut, 3. double-end-stud pressure sensor, 4. pre-tightening gasket, 5. pre-tightening nut, 6. mother nut. Although this pre-tightening method can realize the precise adjustment of pre-tightening force, it cannot achieve automatic adjustment.

Like the gasket method, the thread method, the tooth difference method and the spring method are difficult to achieve timely adjustment of pre-tightening force.

Piezoelectric ceramics can also adjust ball screw pre-tightening [6–11], but with a low stretching strain, energy strain and output force.

Compared with piezoelectric ceramics, GMM's extend-retract strain, output force and energy strain are all much higher [12–15]. Therefore, when it is used for ball screw pre-tightening, the pre-tightening force can be adjusted within a relatively wider range [16], and precise adjustment of pre-tightening force can be achieved simultaneously [17].

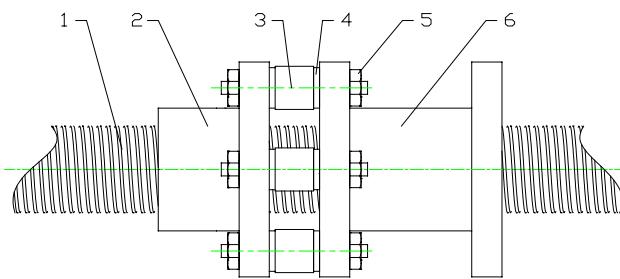
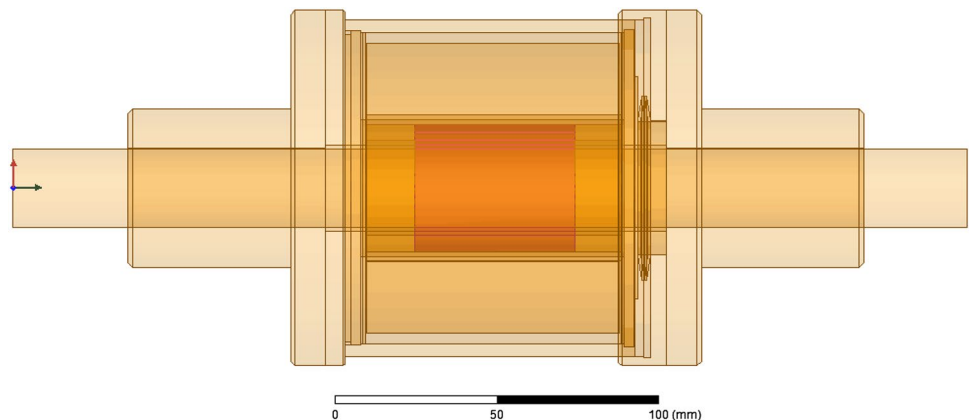


**Fig. 1** Double-nut ball screw that can realize precise adjustment of pre-tightening force

**Fig. 2** Whole structure of the pre-tightening structure composed of hollow cylindrical GMM



## 2.2 Three new giant magnetostrictive structures for double-nut ball screw pre-tightening

### 2.2.1 Pre-tightening structure composed of hollow cylindrical GMM

The whole structure is shown in Fig. 2, where the red part is hollow cylindrical GMM.

Its part-sectioned view is shown in Fig. 3, where 1. nut A, 2. end cap A, 3. cylindrical shell, 4. coil, 5. disk-like yoke iron, 6. end cap B, 7. nut B, 8. disk spring, 9. force sensor, 10. force output link, 11. yoke iron A, 12. inner sleeve, 13. outer sleeve, 14. hollow cylindrical GMM, 15. yoke iron B, 16. coil rack.

It can be seen from Fig. 3 that the pre-tightening structure mainly includes the cylindrical GMM and the excitation coil. The magnetic field generated by excitation coil drives the cylindrical GMM to extend or retract, thus to produce pre-tightening force.

### 2.2.2 Pre-tightening structure composed of three discrete GMM rods

This structure is shown in Fig. 4, where 1. screw, 2. screw nut A, 3. locknut, 4. round nut, 5. pre-tightening structure composed of one discrete cylindrical GMM, 6. force sensor, 7. screw nut B. Each rod in this structure is an indispensable substructure. Its part-sectioned view is shown in Fig. 5, where 1. flat key, 2. screw nut B, 3. heat insulating layer, 4. end cap A, 5. end A of force sensor, 6. force sensor, 7. end B of force sensor, 8. sleeve, 9. disk spring, 10. ejector rod, 11. excitation coil, 12. coil rack, 13. end cap B, 14. locknut, 15. Terfenol-D rod, 16. screw nut A, 17. screw.

**Fig. 3** Part-sectioned view of the pre-tightening structure composed of hollow cylindrical GMM

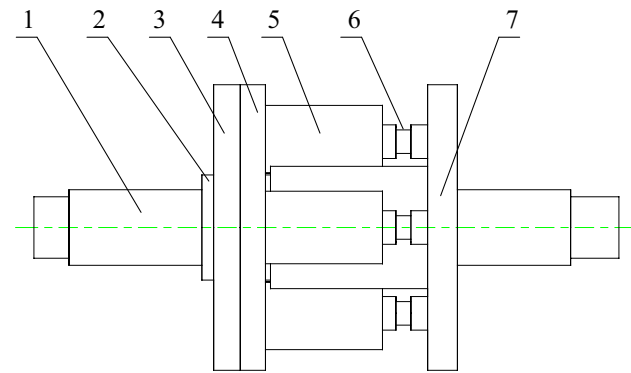
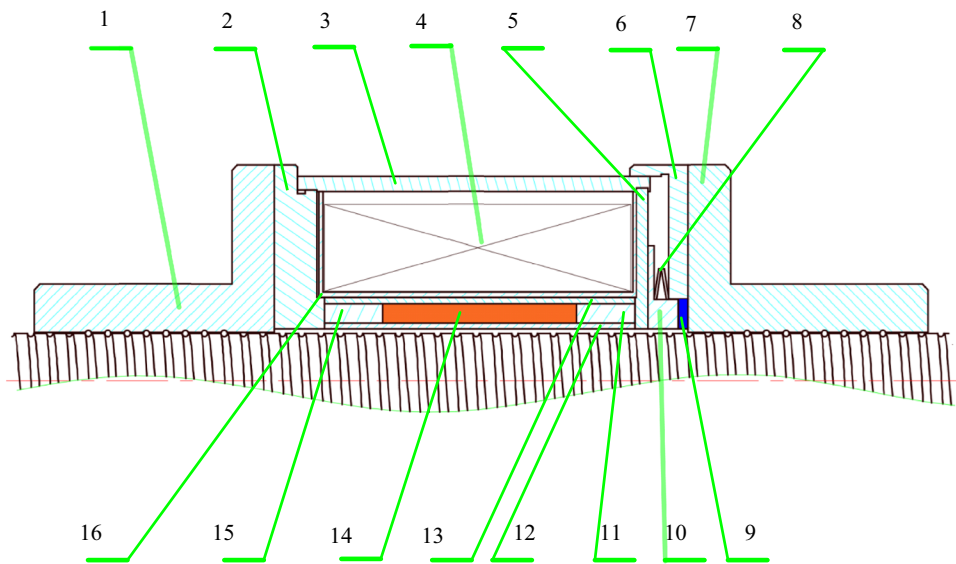


**Fig. 4** Pre-tightening structure composed of three discrete GMM rods

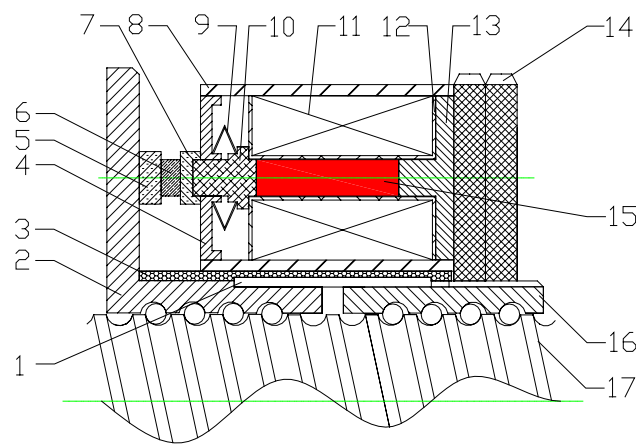


**Fig. 5** Part-sectioned view of one discrete GMM rod

### 2.2.3 Giant magnetostrictive pre-tightening structure with hinge-levers

The giant magnetostrictive pre-tightening structure with hinge-levers is shown in Fig. 6, where 1. soleplate, 2. hinge-lever A, 3. screw nut, 4. screw, 5. hinge-lever B, 6. the giant magnetostrictive structure composed of one GMM rod.

With the help of fixed hinge and live hinge, the hinge-levers use the lever principle to realize the increase, decrease and transmission of force. The output force of giant magnetostrictive device is magnified by hinge-lever A and then transmitted by hinge-lever B.

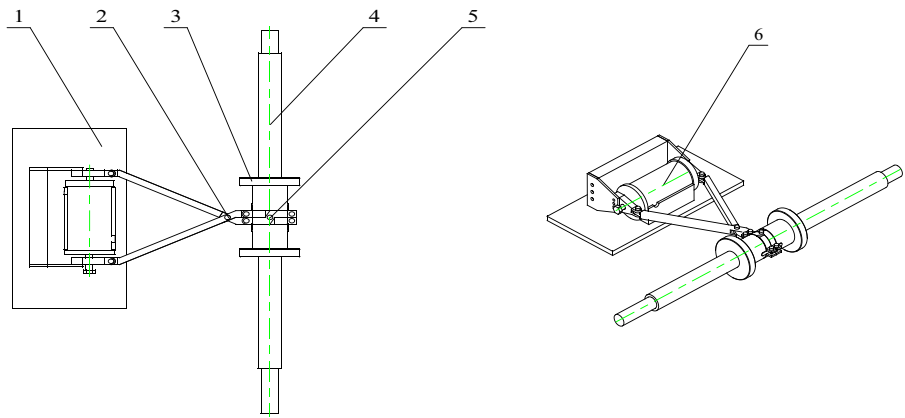
## 2.3 Characteristics of the three new structures

### 2.3.1 Demands for GMM

In structure 2.2.1, GMM needs to be machined into a hollow cylinder, while GMM is a difficult-to-machine material with high processing costs. In addition, for ball screw with larger diameter, a larger-diameter GMM is needed, but according to current production capacity, the diameter of GMM rod can only reach 70 mm, so the diameter of screw used is restricted.

In structure 2.2.2, GMM needs to be machined into rod, which is easy to machine. But its structure is complex with three rods, and it is heavy enough to deform the screw. In addition, the performance of the three rods may be inconsistent with each other, which makes it difficult for them to output completely equal force.

**Fig. 6** Giant magnetostrictive pre-tightening structure with hinge-levers



In structure in 2.2.3, like in structure in 2.2.2, GMM rod is needed.

**2.3.2 Energy distribution in different GMM**

Simulation conditions of hollow cylindrical GMM are set as: The coil’s inner radius is 23.219 mm, outer radius is 45.719 mm, and the coil length is 79 mm. The hollow cylindrical GMM’s inner diameter is 30 mm, outer diameter is 40 mm, and the length is 50 mm. The ampere-turns is 3074 A, and the magnetic field strength is 34.4 KA/m. The energy distribution of hollow cylindrical GMM is shown in Fig. 7.

The energy is mainly distributed in the GMM and the screw. If the screw consumes too much energy, the screw will deform due to the heat.

Simulation conditions of GMM rod are set as: The coil’s inner radius is 9.219 mm, outer radius is 31.719 mm, and

the coil length is 79 mm. GMM rod diameter is 10 mm. The ampere-turns is 3074 A, and the magnetic field strength is 34.4 KA/m. The energy distribution of the GMM rod is shown in Fig. 8.

The energy is mainly distributed in the GMM rod. The energy distribution at the geometrical center lines of the GMM rod and the hollow cylindrical GMM is shown in Fig. 9.

From Figs. 7, 8 and 9, it can be seen that at the same magnetic field strength, the energy distribution in GMM rod is more uniform than in the hollow cylindrical GMM.

**2.3.3 Comparison of the three new structures**

After comparing the three structures, it is found that the giant magnetostrictive pre-tightening structure with hinge-levers is superior to the other two. Its production and processing cost is low, its weight will not affect the screw, no

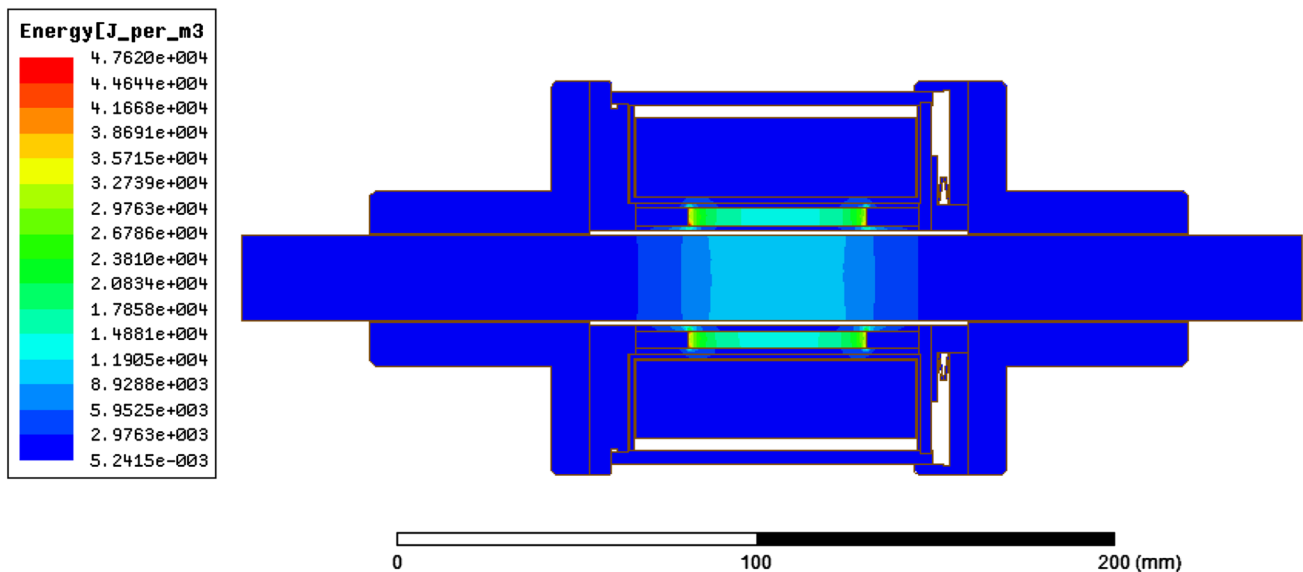


**Fig. 7** Energy distribution in pre-tightening structure composed of hollow cylindrical GMM

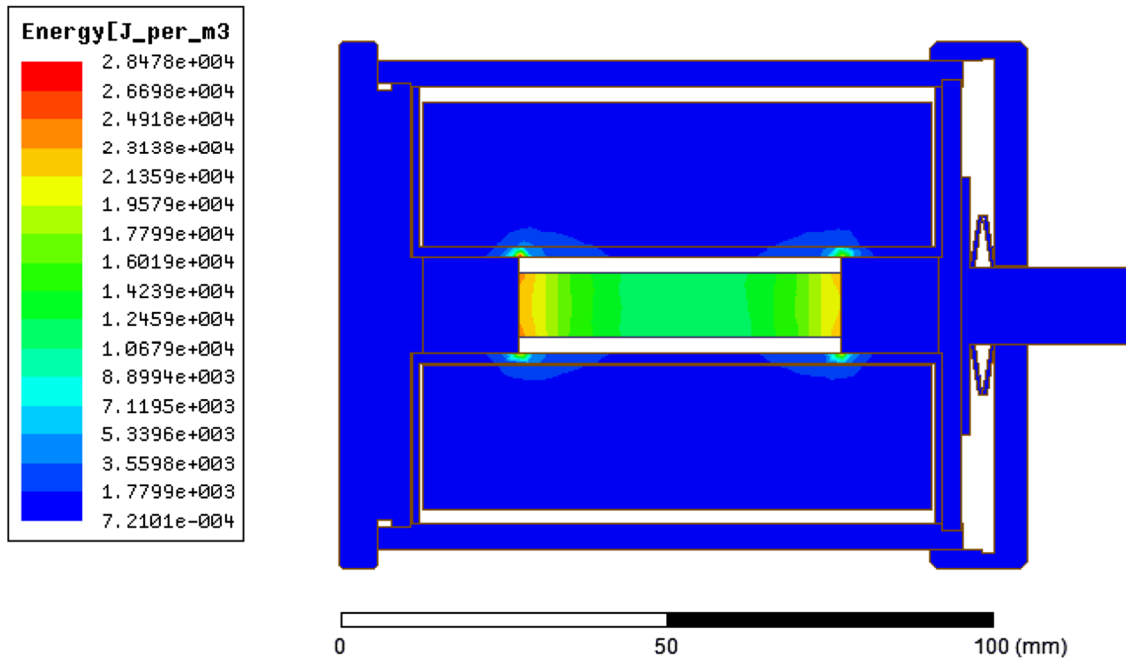


**Fig. 8** Energy distribution in cylindrical GMM

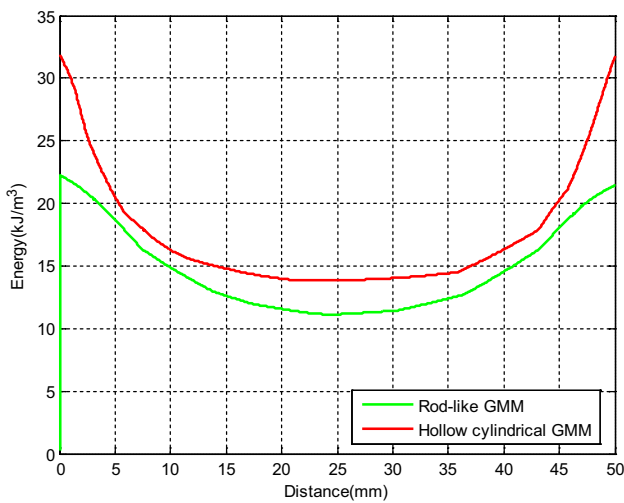


**Fig. 9** Energy distribution in hollow cylindrical and rod-like GMM

**Table 1** Parameters of coil, load and actuator

Name of parameter	Expressed as	Object
Coil turns	$N$	Coil
Coil length	$l_{\text{coil}}$	Coil
Input current	$I$	Coil
Equivalent damping coefficient	$C_l$	Load
Equivalent mass	$M_l$	Load
Equivalent stiffness coefficient	$K_l$	Load
Output force	$F_A$	Cylindrical GMM

more energy is consumed on the screw, and the GMM rod has a more uniform energy distribution than the hollow cylindrical GMM at the same magnetic field intensity.

### 3 Dynamics analysis of the giant magnetostrictive structure

Parameters of the giant magnetostrictive structure are listed in Table 1.

Dynamics model is the base of structure analysis [18, 19]. The giant magnetostrictive structure’s mechanical model is shown in Fig. 10.

Parameters of the GMM rod are listed in Table 2. The rod-like GMM’s load (including the disk spring, the ejector rod, tail mass) is regarded as a mass-spring-damper load, as shown in Fig. 10. The displacement, velocity and acceleration of the rod-like GMM’s one end remain zero during the total moving process, and the other end’s displacement  $y$ , velocity  $\dot{y}$  and acceleration  $\ddot{y}$  are the same as its load.  $\sigma_0$  is the pre-stress that the disk spring acts on GMM rod.

GMM rod can be regarded as a mass-spring-damper with a single degree of freedom in longitudinal direction. The mechanical model of GMM rod is shown in Fig. 11.

$l_{\text{coil}}$  is slightly larger than  $l_{\text{rod}}$  in the giant magnetostrictive structure. The internal magnetic field intensity  $H$ , the magnetic induction  $B$ , the strain  $\varepsilon$  and stress  $\sigma$  in GMM rod are supposed to be uniform. Here,  $\varepsilon$  is the total magnetic hysteresis nonlinear strain under piezomagnetic

**Fig. 10** Giant magnetostrictive structure’s mechanical model

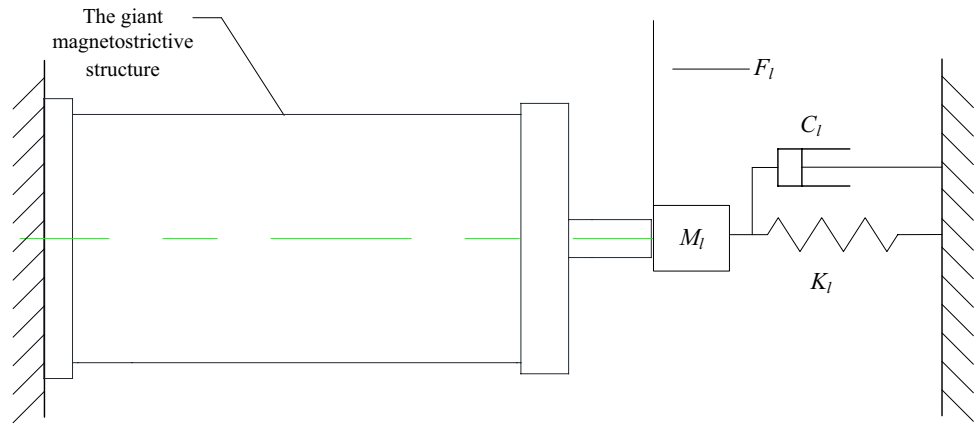


**Table 2** Parameters of the GMM rod

Name of parameter	Expressed as
Cylindrical GMM diameter	$d$
Cylindrical GMM length	$l_{rod}$
Cross-sectional area	$A_{rod}$
Internal damping coefficient	$C_D$
Density	$\rho$
Equivalent stiffness coefficient	$K_{rod}$
Equivalent damping coefficient	$C_{rod}$
Equivalent mass	$M_{rod}$
Magnetic strain	$\lambda$
Output force	$F$
Output displacement	$y$
Pre-stress acting on GMM	$\sigma_0$
Load acting on GMM	$F_l$

$$F_l = (M_l \ddot{y} + C_l \dot{y} + K_l y). \tag{2}$$

According to Newton’s second law, the GMM rod output force is:

$$F = -(F_l + \sigma_0 A_{rod}). \tag{3}$$

Substitute Formula (1) and (2) into Formula (3),

$$\sigma A_{rod} = -(M_l \ddot{y} + C_l \dot{y} + K_l y + \sigma_0 A_{rod}). \tag{4}$$

Considering the GMM rod’s mass and damping [20], its strain equation can be written as:

$$\varepsilon = \sigma / E^H + \lambda - (C_D / E^H) \dot{\varepsilon} - \frac{\rho l_{rod}^2 / E^H}{3} \ddot{\varepsilon}, \tag{5}$$

$$y = \varepsilon l_{rod}, \tag{6}$$

Then the giant magnetostrictive structure’s dynamics differential equation under the action of  $\lambda$  and  $\sigma_0$  can be obtained by substituting Formula (4), (5) and (6):

$$M \ddot{y} + C \dot{y} + Ky = A_{rod} E^H \lambda - \sigma_0 A_{rod}, \tag{7}$$

where  $M = M_{rod} + M_l$ ,  $C = C_{rod} + C_l$ ,  $K = K_{rod} + K_l$ ,  $M_{rod} = \rho l_{rod} A_{rod} / 3$ ,  $C_{rod} = C_D A_{rod} / l_{rod}$ ,  $K_{rod} = A_{rod} E^H / l_{rod}$ .

Laplace transform is taken in Formula (7) to obtain the giant magnetostrictive structure output displacement:

$$y = \frac{1}{Ms^2 + Cs + K} (A_{rod} E^H \lambda - \sigma_0 A_{rod}). \tag{8}$$

$F_A$  and  $F_l$  are opposite to each other in direction, but equal in value, that is,

$$F_A = (M_l s^2 + C_l s + K_l) y. \tag{9}$$

Substitute Formula (8) into Formula (9),

$$F_A = \frac{M_l s^2 + C_l s + K_l}{Ms^2 + Cs + K} (A_{rod} E^H \lambda - \sigma_0 A_{rod}). \tag{10}$$

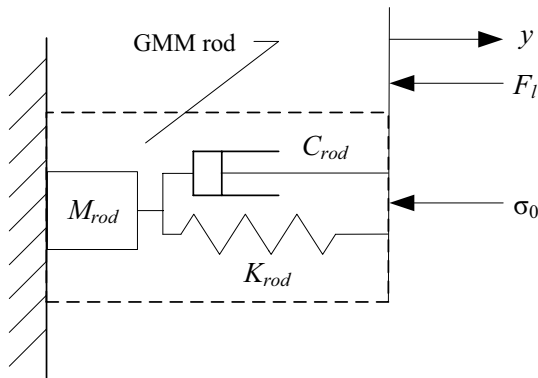


**Fig. 11** Mechanical model of GMM rod

effect, and such factors as vortices, dynamics mechanical properties and magnetic field and stress higher order terms are not considered.

$$F = \sigma A_{rod}, \tag{1}$$

It can be seen from Formula (10) that the giant magnetostrictive structure output force is coupled with the magnetic strain  $\lambda$  and stress  $\sigma_0$ , and the magnetic strain  $\lambda$  is coupled with the current  $I$  in the coil. The output force can be changed by changing the input current.

#### 4 Pre-tightening experiment of giant magnetostrictive structure with hinge-levers

The pre-tightening force adjustment of the above three kinds of structures is shown in Fig. 12. The microcontroller sends out the control signal to the controllable constant current source through DAC, the controllable constant current source outputs the corresponding current to the excitation coil to adjust the magnetic field intensity of GMM, and meanwhile the changes of driving magnetic field will make the GMM extend or retract, thus to obtain the pre-tightening force between screw and nut by the output link. The force sensor is used to measure the pre-tightening force.

Here, we use the giant magnetostrictive structure with hinge-levers to do pre-tightening force experiment and the experiment table is shown in Fig. 13, where 1. PC, 2. stabilized current supply for giant magnetostrictive device, 3. DC power for force sensor, 4. ball screw, 5. nut A, 6. force sensor, 7. hinge-lever B, 8. nut B, 9. hinge-lever A, 10. the giant magnetostrictive structure, 11. transmitter of the force sensor, 12. data acquisition unit.

A digital direct current source is adopted, with a continuously adjustable output voltage 0–30 V and output current –10 to 10 A. A piecewise linear current is applied to the giant magnetostrictive structure, GMM outputs a force under magnetostriction effect, and then the force is transmitted to the screw and nuts by hinge-levers A and B. The pre-tightening force between screw and nuts measured by the sensor is shown in Fig. 14.

It can be seen from the experiment results that the pre-tightening force changes with the current. When current changes from –3 to 3 A, the max output pre-tightening force may reach 1892.87 N.

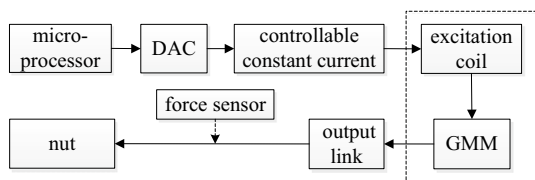


Fig. 12 Pre-tightening force adjustment process

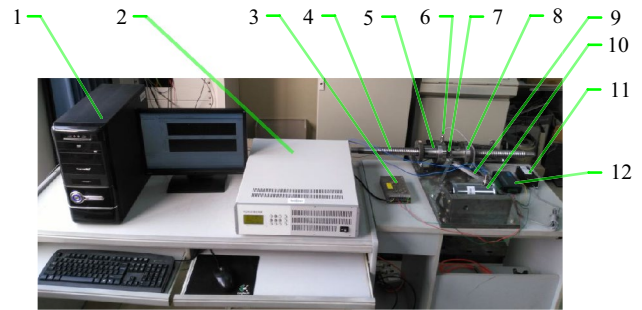


Fig. 13 Pre-tightening force experiment of ball screw

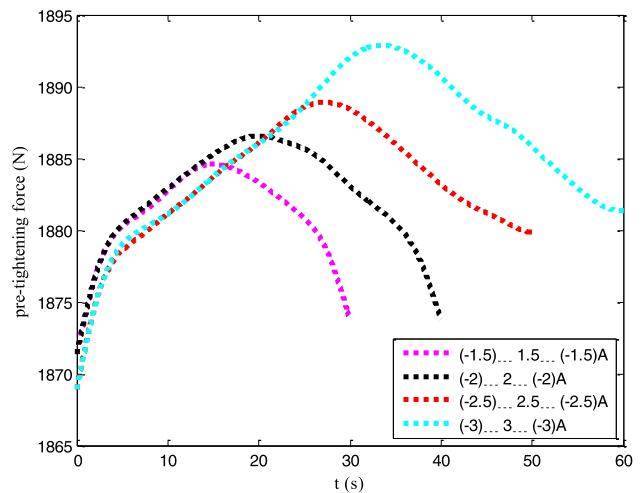


Fig. 14 Pre-tightening force and current

#### 5 Conclusion

In this paper, to achieve double-nut ball screw automatic pre-tightening, three new types of giant magnetostrictive pre-tightening structures are introduced. The characteristics of these three structures are analyzed by electromagnetic field simulation, and their working principles are stated. A dynamics model is established to analyze the factors affecting the pre-tightening force. The mechanical and electrical coupling experiments were carried out and the results show that using the giant magnetostrictive device to adjust the ball screw pre-tightening force is feasible. In order to obtain a better ball screw pre-tightening effect, the giant magnetostrictive structure parameters will be optimized in the future research to improve its mechanical–electrical coupling performance.

**Acknowledgements** This work is supported by National Natural Science Foundation of China (Grant No. 51475267).

## References

1. Fleischer J, Herder S (2012) Adaptronic ball screw for the enhancement of machine precision. *Procedia Cirp* 1:621–626
2. Verl A, Frey S (2010) Correlation between feed velocity and preloading in ball screw drives. *CIRP Ann* 59:429–432
3. Song XC, Jian S, Chen MY, Li YF (2012) “Research on axial stiffness of the double-nut ball screw mechanism”, MEMS-12
4. Wei CC, Liou WL, Lai RS (2012) Wear analysis of the off-set type preloaded ball–screw operating at high speed. *Wear* 292:111–123
5. Feng GH, Pan YL, Feng GH, Pan YL (2012) Investigation of ball screw preload variation based on dynamic modeling of a preload adjustable feed-drive system and spectrum analysis of ball-nuts sensed vibration signals. *Int J Mach Tools Manuf* 52:85–96
6. Henriksen AD, Rizzi G, Hansen MF (2016) Planar Hall effect bridge sensors with NiFe/Cu/IrMn stack optimized for self-field magnetic bead detection. *J Appl Phys* 119:093910
7. Jakes P, Erdem E, Eichel RA, Jin L (2011) Position of defects with respect to domain walls in Fe<sup>3+</sup>-doped Pb[Zr<sub>0.52</sub>Ti<sub>0.48</sub>]O<sub>3</sub> piezoelectric ceramics. *Appl Phys Lett* 98:072907
8. Hong CC (2013) Application of a magnetostrictive actuator. *Mater Des* 46:617–621
9. Hockel JL, Wu T, Carman GP (2011) Voltage bias influence on the converse magnetoelectric effect of PZT/terfenol-D/PZT laminates. *J Appl Phys* 109:064106
10. Pislaru-Danescu L, Morega AM, Morega M (2011) “A novel magnetostrictive injection actuator based on new giant magnetostrictive materials”, International Symposium on Advanced Topics in Electrical Engineering, pp. 1–6
11. Engelberth T, Apprich S, Friedrich J, Coupek D, Lechler A (2015) Properties of electrically preloaded rack-and-pinion drives. *Prod Eng Res Devel* 9:269–276
12. Sheykholeslami M, Hojjat Y, Ghodsi M, Kakavand K, Cinquemani S (2015) Investigation of  $\Delta E$  effect on vibrational behavior of giant magnetostrictive transducers. *Shock Vib* 2015:1–9
13. Yoshioka H, Shinno H, Sawano H (2013) A newly developed rotary-linear motion platform with a giant magnetostrictive actuator. *CIRP Ann* 62:371–374
14. Witthauer A, Kim GY, Faidley LA, Zou Q, Wang Z (2014) Design and characterization of a flexensional stage based on Terfenol-D actuator. *Int J Precis Eng Manuf* 15:131–137
15. Davino D, Giustiniani A, Visone C (2012) The piezo-magnetic parameters of Terfenol-D: an experimental viewpoint. *Physica B* 407:1427–1432
16. Witthauer A, Kim GY, Faidley LA, Zou Q, Wang Z (2014) Design and characterization of a flexensional stage based on Terfenol-D actuator. *Int J Precis Eng Manuf* 15:131–137
17. Bucht A, Sosa IND, Pagel K, Junker T, Drossel WG (2012) “Self-controlling structures using thermal shape memory alloys”. In: *Frontiers in Computer education*, pp. 1119–1126
18. Lassila TM, Stevanella M, Votta E, Redaelli A, Deparis S (2012) Multiscale fluid-structure interaction simulation of anatomically correct left ventricle fluid dynamics with fictitious elastic structure regularization. *Psychosomatics* 17:10–13
19. Yoo B, Hirata K (2010) Analysis method for giant magnetostrictive material based actuator using FEM. *IEEJ Trans Ind Appl* 130:721–727
20. Juhász L, Maas J, Borovac B (2011) Parameter identification and hysteresis compensation of embedded piezoelectric stack actuators. *Mechatronics* 21:329–338